Determination of impurities in antique silver objects for authentication by laser ablation inductively coupled plasma mass spectrometry (LA-ICP-MS)

JAAS Journal of Analytical Atomic Spectrometry

W. Devos, Ch. Moor* and P. Lienemann

Swiss Federal Laboratories for Materials Testing and Research (EMPA), Überlandstrasse 129, CH-8600 Dübendorf, Switzerland

Received 4th January 1999, Accepted 25th February 1999

In addition to visual characteristics, a less manipulable criterion for authenticity verification of silver antiques is given by trace and minor element patterns in the silver alloy. The analytical method used to analyse precious silver antiques should not visibly damage the object and should enable the determination of impurities in the ppm–0.5% range. Using laser ablation inductively coupled plasma mass spectrometry (LA-ICP-MS), visible damage can be restricted to an acceptable minimum. Because most antique silver objects are too large to fit into a normal laser ablation cell, an alternative cell design was used that allows a direct, virtually non-destructive analysis of entire antique silver objects. This cell is placed upon the object to be analysed. A micro-amount of the object is then ablated through an aperture in the bottom of the cell. The 100 μm wide craters are almost invisible on an antique silver object. The analytes Zn, Cd, Sn, Sb, Au, Pb and Bi were measured. Signals were normalized to the Ag signal and silver standard materials were used for external calibration. The crater-to-crater repeatability of the normalized signals in a homogeneous silver sample was below 10% RSD ($n=3$) for most elements. Detection limits lie within the sub-ppm to 2 ppm range. The accuracy was validated with comparative ICP-MS measurements after digestion and with X-ray fluorescence (XRF) measurements. The analysis of eight antique silver objects, including one forgery, illustrates the application of the method.

Introduction

Various criteria are available to verify if an antique silver object is authentic or a forgery. A trained expert in silver antiques may be able to identify forgeries by a careful visual study of stylistic characteristics, hallmarks, fabrication technique and signs of wear. However, a malevolent silversmith with sufficient expertise can manipulate these criteria so as to make a forgery look real, even to a trained eye. An additional criterion much more difficult to manipulate is given by the chemical composition of the silver alloy. In addition to the main constituents of silver (75–95%) and copper (5–25%), a silver alloy contains minor or trace impurities typical of the metallurgical manufacturing and refinement process of the silver, such as Zn, Cd, Sn, Sb, Au, Pb and Bi. Silver refinement has undergone fundamental changes during the past centuries, especially in the 19th century, as the introduction of the Parkes process around 1850, followed by electrolytic refinement in 1884, led to much lower contents of Zn, Sn, Sb, Au, Pb and Bi. Cd, on the contrary, only discovered in 1817, has temporarily been used as an additive in 20th century silver solders and special silver alloys and is a clear indication of a modern silver alloy.[1,2] As it was not until the latter part of the 19th century that collecting antique silver came into vogue, most fake silver objects stem from that period on. Therefore 1850 is a significant date to distinguish forgeries from earlier genuine silver antiques.

It is evident that any analytical method used for authenticity verification of often precious antique silver objects should be either non-destructive or require an extremely small sample amount. Furthermore, it should allow the determination, preferably simultaneously, of the relevant elements in a concentration range from a few μg g^{-1} to about 0.5%.

Classical methods for direct solid sample analysis, such as X-ray fluorescence (XRF) analysis, scanning electron microscopy with an energy-dispersive X-ray detection system (SEM-EDXRF) or electron probe microanalysis (EPMA), are fully non-destructive, but lack sensitivity in the lower μg g^{-1} range. Furthermore, most antique silver objects are too large to be fitted into the sample chambers commonly used with these techniques.

Wet analytical techniques, *e.g.*, atomic absorption spectrometry (AAS) and inductively coupled plasma mass spectrometry (ICP-MS) of solutions, require acid digestion of the Ag–Cu alloy. This is particularly troublesome if Au also has to be determined, as traces of Au are only partially soluble in nitric acid, whereas Ag will precipitate as silver chloride in *aqua regia*, giving rise to losses of trace elements due to coprecipitation. It is possible to keep Ag in solution as chloride complexes with a carefully balanced mixture of nitric and hydrochloric acid, but this demands quite a lot of experience and time. To overcome this problem, Hinds[3] used solid sampling graphite furnace AAS (GFAAS) for the determination of Au, Pd and Pt in high purity silver, and Moor *et al.*[4] reported the application of solid sampling electrothermal vaporization ICP-MS (ETV-ICP-MS) to determine Au and other impurities in silver alloys. In order to allow practical sample handling, both techniques require in practice at least 50–100 μg of sample. Coupling solid sample introduction techniques to ICP-MS has a powerful advantage over solid sampling GFAAS in that it offers a quasi-simultaneous multi-element analysis in one signal acquisition run.

In recent years, laser ablation (LA) has gained increased popularity as a solid sample introduction technique to ICP-MS, thanks to its low detection limits, its wide linear dynamic range, its spatial resolution and its low consumption

of sample material.[5–9] The benefits of LA-ICP-MS in trace analysis of silver and gold materials for assessing the provenance of stolen gold,[10] for prospecting purposes[11] and for the determination of impurities in pure coinage silver and gold[12] have been reported.

In LA-ICP-MS, a sample is usually mounted into a relatively small, closed laser ablation cell, in which the ablation process takes place and through which a carrier gas stream flows to transport the ablated material to the ICP-MS. Objects larger than a few centimetres, however, *e.g.*, the silver antiques under study here, require the removal of a fragment of the object in order to fit into a normal laser ablation cell and can thus be analysed only indirectly. For a high quality piece of antique this is unacceptable. Special cell designs have been proposed by Arrowsmith and Hughes[13] and Günther[14] which consist of a cell that encloses the plume of ablated material but not the sample. In this work, an alternative cell design was used in combination with a home-built autofocus system, allowing the direct analysis of entire antique silver objects by LA-ICP-MS. Quantitative information was obtained using matrix matched standards.

Experimental

Instrumentation

An Elan 6000 ICP-MS (Perkin-Elmer SCIEX, Thornhill, Ontario, Canada) was used in combination with a Laser Sampler Model 320 (Perkin-Elmer SCIEX, Thornhill, Ontario, Canada). Measurements were performed in the dual detection mode of the Elan 6000, which offers the measurement of pulse-counting and analogue signals simultaneously.[15] The Laser Sampler Model 320 was modified by adding a home-built autofocus system.[16] The laser used in this work is an Nd : YAG laser (Spectra-Physics, Darmstadt, Germany), operated at 532 nm. The area of ablation can be observed by a video camera.

An alternative laser ablation cell was used to analyse entire antique silver objects directly, *i.e.*, without the need to remove a fragment from the object. This cylindrical borosilicate glass cell ($r = 2.1$ cm; $h = 1.7$–2.4 cm) has a flat exchangeable Plexiglas bottom with a central aperture of 5 mm, 10 mm or 20 mm, and is placed upon the object to be analysed (Fig. 1). Part of the object is then ablated by the laser beam through the aperture. The cell is continuously flushed with a carrier gas (argon) *via* a lateral inlet and outlet tube to transport the ablated material to the ICP-MS. To prevent the Ar carrier gas, and therewith the ablated material, from escaping out of the cell through the aperture, modelling plasticine is applied between the cell and the object, around the aperture. For flat objects, a flat rubber sealing-ring can be used instead. For the analyses in this study, the bottom disc with a 5 mm aperture was used.

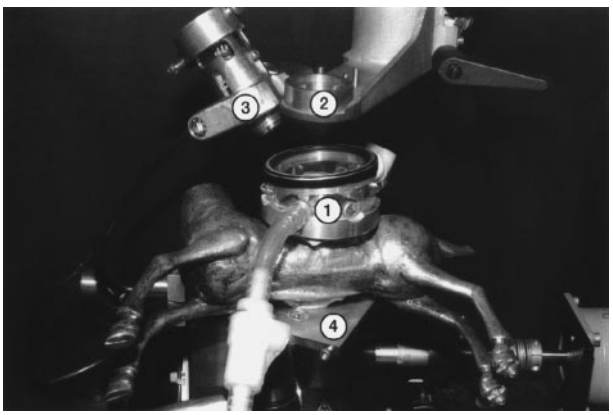

Fig. 1 The alternative laser ablation cell used in this work, placed upon a silver object: 1, laser ablation cell; 2, focusing lens; 3, autofocus; 4, supporting platform.

A supporting platform, adjustable in three dimensions and mounted on the Laser Sampler Model 320 supporting block with its three stepping motors, allows the aperture of the cell and, consequently, the area of interest on the object to be exactly positioned under the focusing lens. The autofocus system then automatically adjusts the surface of the object within the focal plane of the laser beam.

Laser analysis and signal processing

The carrier gas flow rate was optimized for maximum integrated signals with a silver standard material. A short bivariate optimization study was carried out for the number of laser pulses per analysis point and the excitation lamp energy in order to obtain craters of a suitable size. By increasing the excitation lamp energy, which directly influences the laser beam energy, wider and deeper craters are produced, whereas increasing the number of shots only produces deeper craters. The operating conditions of the ICP-MS and the laser sampler are listed in Table 1. The laser was focused on the sample surface. Analysis points were chosen a few millimetres apart.

To correct for differences in ablation efficiency between analysis points, ^{107}Ag was used as an internal standard. This requires the silver content of the samples and external standards to be approximately known. The external standards used in this work (see below) contained between 99.4 and 100% silver. Unless given by other sources, a silver content of 84% was used as an approximation of the silver content in the alloy of antique silver objects. Some commonly used antique alloys were 12/16 (*i.e.*, m/m Ag/alloy ratio), 13/16, 14/16 and 15/16 silver (1/16 = 1 'Lot'), Sterling silver (92.5% fine silver) and 9/12, 10/12 and 11/12 silver (1/12 = 1 'denier' or 'dinero').[17–19] Generally, the silver content of antique and modern alloys for silverware lies between about 75% and 95%. Thus, using an approximation of 84% silver for internal standardization introduces a supplementary relative uncertainty of, at most, $\pm 12\%$, which is still acceptable for authentication purposes.

Based on the literature[1] and preliminary experiments with solid sampling ETV-ICP-MS and conventional ICP-MS,[4] the following isotopes were chosen for analysis: ^{66}Zn, ^{107}Ag, ^{111}Cd, ^{117}Sn, ^{121}Sb, ^{197}Au, ^{208}Pb and ^{209}Bi. The transient signals were

Table 1 Operating conditions for the ICP-MS and the laser sampler

ICP-MS	
Rf power/W	1050
Gas flow rates/l min^{-1}	
Plasma gas	15
Auxiliary gas	0.8
Carrier gas	1.0
Lens setting	Autolens mode (variable)
Points per peak	1 (at peak maximum)
Measuring mode	Peak hopping
Isotopes measured	^{66}Zn, ^{107}Ag, ^{110}Cd (dummy), ^{111}Cd, ^{117}Sn, ^{121}Sb, ^{197}Au, ^{208}Pb, ^{209}Bi
Dwell time/ms	10; ^{111}Cd and ^{121}Sb: 50
Sweeps per reading	1
Readings per replicate	91
Detector mode	Dual (pulse counting and analogue)
Laser sampler	
Mode	Q-switch
Q-switch time/μs	240
Excitation lamp energy/J	45
Pulse frequency/Hz	10
Number of pulses/analysis point	60
Focus	On sample surface (autofocus)

integrated over a period of 20 s after the laser had started firing, thus covering the entire analyte signals, while allowing the silver signal to decrease to about 1% of its maximum intensity. A blank correction was carried out by subtracting the Ar gas blank signal, integrated over the same period of time and measured with the laser running but the laser beam path blocked.

Calibration

To obtain similar ablation conditions for external standards and samples, matrix-matched standards or standard materials with chemical and physical properties very similar to the samples are preferred in laser ablation analysis. Three silver calibration standards were purchased from VEB Bergbau- und Hüttenkombinat (Freiberg, Germany), containing the elements of interest at known concentration levels of around 500 μg g^{-1} ('Ag500'), 100 μg g^{-1} ('Ag100') and 10 μg g^{-1} ('Ag10') respectively. As these standards were in the form of 10 cm rods with a diameter of only 7 mm, and were therefore too small to place the cell on, a cross-section was made of each standard after embedding in a Plexiglas resin (*RESINAR F*, Wirtz Buehler, Düsseldorf, Germany).

Analysed objects and cleaning procedure

Eight silver objects, provided by a private antique silverware dealer, were analysed in order to investigate their authenticity. Before analysis, the objects were consecutively cleaned with silver polish to remove any AgS patina, *pro analysi* grade ethanol (Merck, Darmstadt, Germany) and ultrapure water (Milli-Q, Millipore, Bedford, MA, USA).

Comparative analyses by solution ICP-MS and WD-XRF

For comparative analysis by ICP-MS of solutions, four samples of 3–5 mg each were taken from an antique silver alloy and submitted to the following open acid digestion procedure. After dissolving the silver alloy with 1 ml concentrated HNO_3 for *ca.* 10 min in a 100 °C hot-water bath, 3 ml concentrated HCl was added (causing precipitation of Ag as AgCl) to dissolve the remaining undissolved Au, and the solution was left to boil for another 30–60 min. After cooling, the solution was made up to 10 ml with deionized water.

Comparative analyses by wavelength dispersive XRF (WD-XRF) were carried out on a Philips PW1404 (Philips, Almelo, The Netherlands) with a Cr tube for the determination of Sn and Sb and a Philips PW2400 with an Rh tube for the other elements of interest. A sample with a flat geometry was prepared from a piece of an antique object which could be destroyed for analysis. The measurements were calibrated with standards 'Ag100' and 'Ag500'.

Results and discussion

Quasi-non-destructiveness

The laser parameters shown in Table 1 resulted in ablation craters of about 100 μm across (Fig. 2b). Three craters per sample were shot. The craters are small enough to be almost invisible with the naked eye (Fig. 2a) on antique silver, and thus are virtually non-destructive. Although the crater size could easily be reduced further, smaller craters would decrease the relative sensitivity and would be less representative of the silver alloy. From the crater width and depth, the ablated mass per crater was estimated to be roughly about 3 μg. After ablation, sometimes a black discolouration of the silver could be observed around the craters. This discolouration could easily be wiped off with a silver polishing cloth.

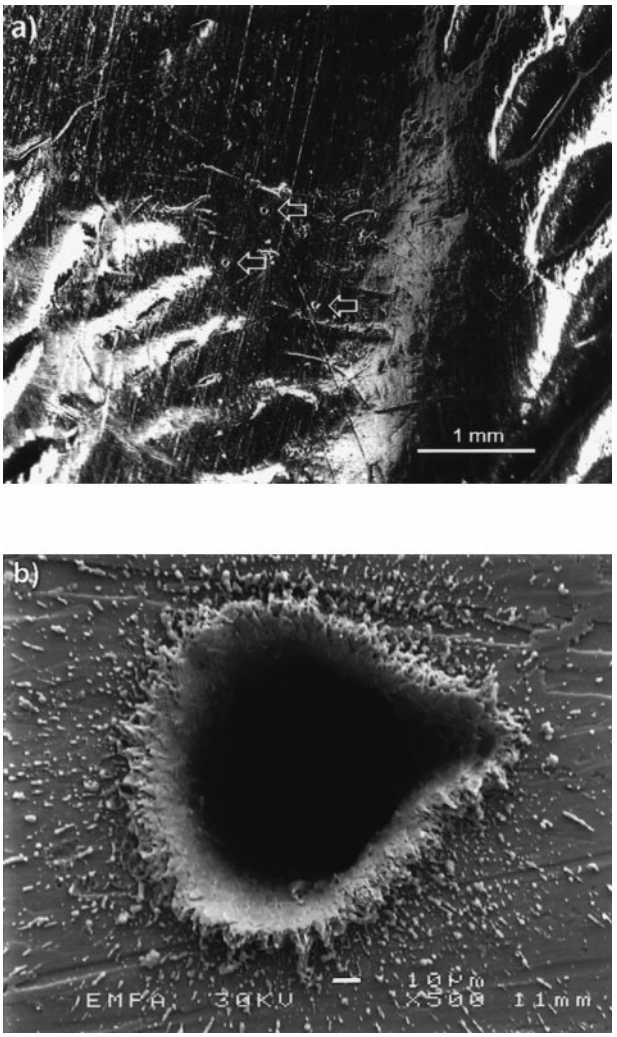

Fig. 2 Details of the silver 'deer' from Fig. 1 after laser ablation analysis. (a) Optical microscopy view. The arrows indicate the ablated craters. (b) Scanning electron microscope (SEM) view of one crater. The diameter of the crater is *ca.* 100 μm. The not quite circular crater shape is possibly due to imperfect optical alignment of the home-built frequency doubling upgrade.

Calibration and detection limits

The three calibration standards 'Ag10', 'Ag100' and 'Ag500' were analysed to investigate whether a linear calibration could be obtained with the alternative cell design. The linearity of the calibration graphs is excellent, with correlation coefficients of 0.996 or better (Fig. 3). Furthermore, the fitted calibration lines go almost perfectly through zero, which confirms that the subtraction of an Ar gas blank is an adequate method for blank correction for the given experimental set-up and this type of sample.

The ^{111}Cd signal initially gave rise to a problem. When ^{111}Cd was measured immediately after ^{107}Ag in the peak hopping sequence, a steady state signal instead of the normal transient signal could be observed at mass 111, which completely masked the transient ^{111}Cd signal for the standard with the lowest Cd concentration ('Ag10': 8.3 μg g^{-1}). This resulted in far too high a signal for Cd in the Ag10 standard. The constant ^{111}Cd signal abruptly dropped to background level at the point where the ^{107}Ag signal had decreased to about 10^7 counts per second (Fig. 4a). This phenomenon was reproducible and was probably caused by a memory effect in the discrete dynode electron multiplier or the electronics of the detection system, due to the high count rates for ^{107}Ag. Introducing a 'dummy' mass between ^{107}Ag and ^{111}Cd, *e.g.*,

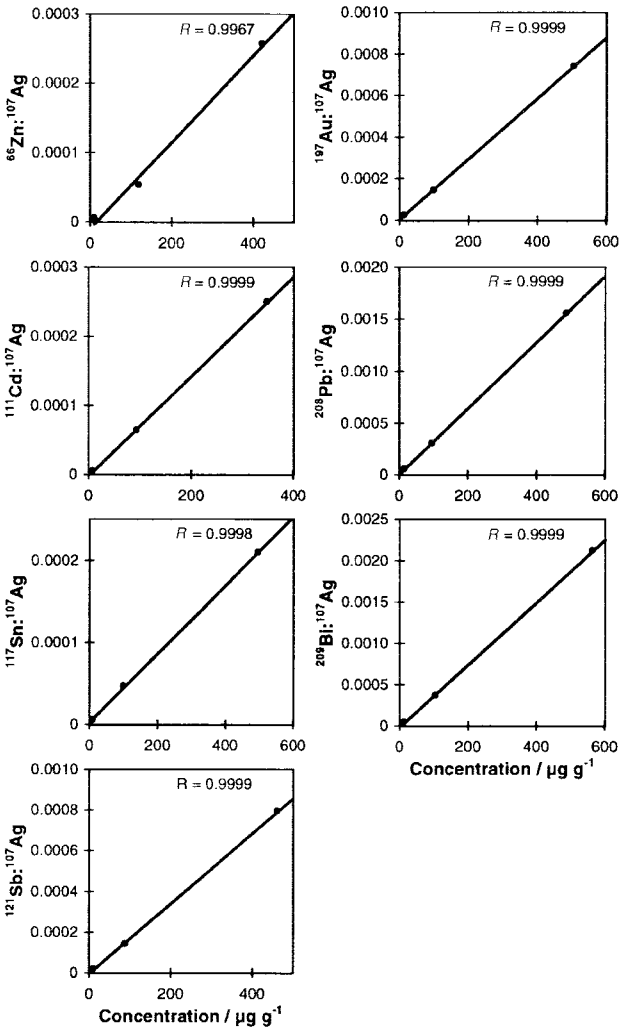

Fig. 3 Calibration graphs of the integrated signal intensity of the isotope monitored ratioed to the integrated Ag signal intensity for the three solid silver calibration standards (VEB Bergbau- und Hüttenkombinat, Freiberg, Germany).

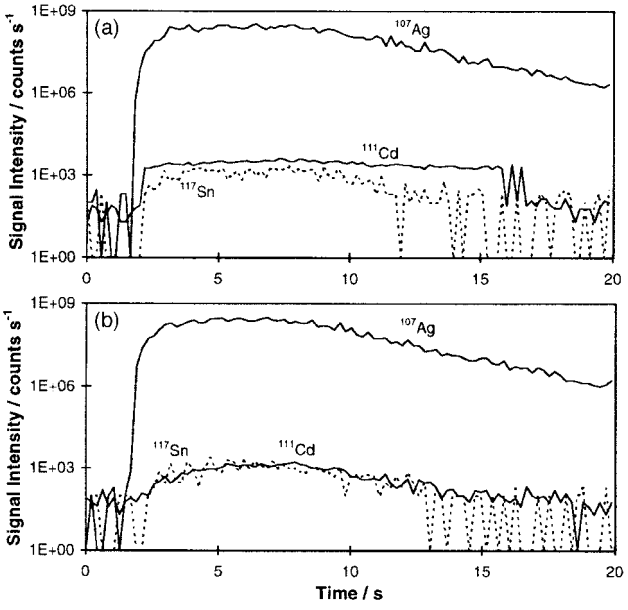

Fig. 4 Transient ^{111}Cd signal intensity for standard 'Ag10' measured without ^{110}Cd (a) and with ^{110}Cd (b) as dummy isotope. The ^{107}Ag and the ^{117}Sn signal profiles are given for comparison.

^{110}Cd, solved the problem and resulted in a normal transient signal (Fig 4b) and a linear calibration curve for ^{111}Cd (Fig. 3).

The detection limits for the elements measured, calculated as 3σ from three Ar blank replicates, lie between 0.06 ppm (Pb and Bi) and 1.6 ppm (Zn).

Accuracy and repeatability

The linearity of the calibration lines based on the solid silver calibration standards suggests a good accuracy, limited by the quality of the standards. Furthermore, an antique silver sample, indicated here as 'Alloy A', was analysed both by LA-ICP-MS and by ICP-MS using a cross-flow nebulizer. As shown in Table 2, the results of the two approaches were in fairly good agreement, considering that only three craters were shot. The differences between the corresponding mean values obtained by the two methods are statistically insignificant (95% confidence level *t*-test) for all elements except Au and Bi. The somewhat lower values for these elements with the solution method may be due to incomplete dissolution.

Additionally, the results of laser ablation analysis of another antique silver sample ('Alloy B') were compared with XRF measurements (Table 2). The concentrations of Sb and Cd were below the detection limits of XRF for these elements in this type of matrix. A statistically significant difference between the two methods was observed for the Pb values. The reason for this difference is not clear, but it might be attributed to surface contamination effects during sample preparation for XRF, as the comparison of LA-ICP-MS with solution ICP-MS did not reveal any systematic deviation of LA-ICP-MS for lead. The agreement between LA-ICP-MS and XRF for the other elements was satisfactory in view of the objectives of this study.

The crater-to-crater repeatability ($n=3$) of the analyte signals (ratioed to the Ag signal) is summarized in Table 3 for the measurements of the standards and the two aforementioned antique silver alloys. The uncertainties shown in Table 2 are larger than the RSDs in Table 3 as they were calculated on a 95% confidence level and include the propagated uncertainty of the calibration. For a homogeneous silver alloy, like 'Alloy B', RSDs ($n=3$) well below 10% could be observed. A larger relative uncertainty was found for Cd in this alloy because its signal was only just above the background noise. In other samples, sometimes a spreading up to 30% RSD was seen for some elements, possibly due to inhomogeneity.

Analysis of the antique silverware objects

Finally, eight antique objects dating from the 16th to the 20th century were directly analysed by LA-ICP-MS using the alternative cell design (Table 4). Their provenance is mainly West European, except for one small spoon from the USA. For gilded objects, an area was analysed where the gilding was not applied or where it had worn off.

It can be observed from Fig. 5 that the small spoon from around 1900 and the 20th century meat fork are characterized by relatively low impurity levels, except for Cd in the meat fork. The relatively high Cd concentration in the meat fork is a clear indication (but not a prerequisite) of a 20th century silver alloy (see Introduction).

With the exception of the 'deer' and its matching socle, all objects from before 1850 show generally much higher concentrations of the measured impurities. For the 'deer' and socle, however, the impurity levels are much too low to be consistent with a silver alloy from before 1850. In view of these results, this object is to be regarded as a forgery, probably from the late 19th century. The high value for Au in the 'deer' is most probably due to remaining traces of the gilding. A fine silver determination by ICP-OES after digestion of a 3 mg sample

Table 2 Comparison of LA-ICP-MS ($n=3$) with ICP-MS from solutions after digestion ($n=4$) for silver Alloy A and with WD-XRF ($n=1$) for Alloy B. All values are in $\mu g\ g^{-1}$. The uncertainties, given as 95% confidence intervals, are propagated values, including the uncertainty of the calibration

	Alloy A		Alloy B	
Analyte	LA-ICP-MS	Solution ICP-MS	LA-ICP-MS	WD-XRF
Zn	7100 ± 2300	7500 ± 2400	1700 ± 500	1400 ± 200
Cd	34 ± 10	26 ± 10	< 2	< 200
Sn	290 ± 90	290 ± 60	400 ± 70	580 ± 200
Sb	300 ± 100	300 ± 70	40 ± 20	< 200
Au	2800 ± 500	2200 ± 500	1400 ± 100	1600 ± 200
Pb	2200 ± 1200	1900 ± 300	1900 ± 500	2900 ± 300
Bi	200 ± 100	110 ± 50	120 ± 20	200 ± 100

Table 3 RSDs (%) for the normalized signal ratios ($n=3$) measured in the external standards and in two antique silver alloys. The concentrations ($\mu g\ g^{-1}$) of the analytes are given in parentheses

	RSD (%) (and concentration/$\mu g\ g^{-1}$)				
Analyte	'Ag10'	'Ag100'	'Ag500'	'Alloy A'	'Alloy B'
Zn	17 (9.8)	4 (120)	3 (424)	13 (7100)	6 (1700)
Cd	8 (8.3)	3 (95)	5 (349)	12 (34)	33 (< 2)
Sn	11 (11.5)	13 (101)	2 (497)	12 (290)	4 (400)
Sb	4 (11)	5 (89.2)	3 (463)	18 (300)	5 (40)
Au	31 (13.6)	4 (101)	11 (506)	7 (2800)	2 (1400)
Pb	5 (15.8)	11 (97.6)	1 (489)	22 (2200)	6 (1900)
Bi	5 (14.7)	5 (107)	3 (566)	21 (200)	3 (120)

from the bottom of the socle additionally confirmed a younger age, as a silver content of almost exactly 80% was found. This corresponds to 'silver 800', an alloy that has been used only since the 19th century.

Conclusion

The presented method has been shown to be sufficiently precise and accurate to allow an *ante quem*/*post quem* dating (before or after 1850) of antique silverware. The main advantage of this method over wet techniques or electron probe microanalysis is that relatively large silver objects can be analysed directly without having to take a visible fragment of the object for digestion or in order to fit into a vacuum sample chamber.

Table 4 Description of the antique silverware objects analysed by LA-ICP-MS

Object	Provenance	Date
Fork	Bern (Switzerland)	2nd half 18th century
Fork	Paris (France)	*ca.* 1780
Meat fork	Schaffhausen (Switzerland)	20th century
Small spoon	USA	*ca.* 1900
Spoon	Amsterdam (The Netherlands)	2nd half 18th century
Deer with matching socle (gilded)	Southern Germany	Mid-17th century (?)
Pomegranate beaker (partially gilded)	Southern Germany	1580
Polychromed wooden sculpture of a man (with gilded silver decoration)	Schwäbisch-Gmünd (Germany)	1620

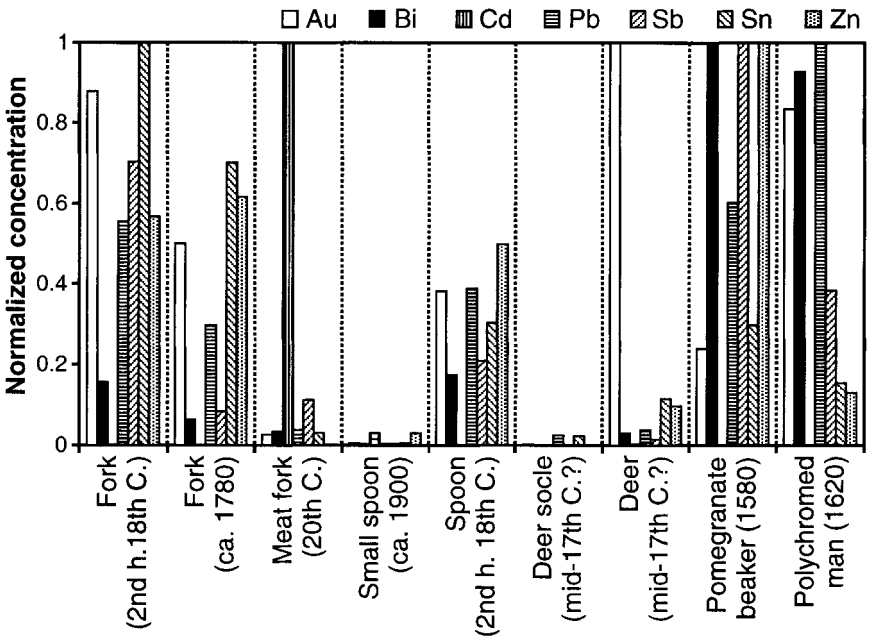

Fig. 5 Impurity patterns in the antique silver objects analysed by LA-ICP-MS. For security reasons, only relative values are shown. The concentration of each element has been normalized to its maximum concentration measured in these objects. The low impurity levels in the 'deer' and the matching socle suggest a post-1850 origin for the objects.

As the craters obtained after firing the laser are almost invisible with the naked eye, the proposed method can be regarded as being virtually non-destructive.

Acknowledgements

The authors wish to thank Mr. Martin Kiener for providing the antique silverware and the very helpful background information.

References

1 E.-L. Richter, *Altes Silber, Imitiert-Kopiert-Gefälscht*, Keyser, Munich, 1983, ch. 15, pp. 245–249.
2 R. D. Mushlitz, in *McGraw-Hill Multimedia Encyclopedia of Science and Technology—'Silver Metallurgy'*, McGraw-Hill, CD-ROM Version 1.0, 1994.
3 M. W. Hinds, *Spectrochim. Acta*, 1993, **48B**, 435.
4 C. Moor, P. Boll and S. Wiget, *Fresenius' J. Anal. Chem.*, 1997, **359**, 404.
5 P. Arrowsmith, *Anal. Chem.*, 1987, **59**, 1437.
6 E. R. Denoyer and K. J. Fredeen, *Anal. Chem.*, 1991, **63**, 445A.
7 L. Moenke-Blankenburg, *Spectrochim. Acta*, 1993, **15**, 1.
8 E. F. Cromwell and P. Arrowsmith, *Anal. Chem.*, 1995, **67**, 131.
9 W. T. Perkins, N. J. G. Pearce and J. A. Westgate, *Geostandards Newsletter—The Journal of Geostandards and Geoanalysis*, 1997, **21**, 175.
10 R. J. Watling, H. K. Herbert, D. Delev and I. D. Abell, *Spectrochim. Acta*, 1994, **49B**, 205.
11 P. M. Outridge, W. Doherty and D. C. Gregoire, *J. Geochemical Exploration*, 1998, **60**, 229.
12 V. V. Kogan, M. W. Hinds and G. I. Ramendik, *Spectrochim. Acta*, 1994, **49B**, 333.
13 P. Arrowsmith and S. K. Hughes, *Appl. Spectrosc.*, 1988, **42**, 1231.
14 D. Günther, Doctoral Thesis, Martin-Luther-University Halle Wittenberg, Halle, Germany, 1990.
15 U. Völlkopf and K. Barnes, *At. Spectrosc.*, 1995, **16**, 19.
16 B. Wanner, Ch. Moor, P. Richner, R. Brönnimann and B. Magyar, *Spectrochim. Acta*, 1999, **54B**, 287.
17 E.-L. Richter, *Altes Silber, Imitiert-Kopiert-Gefälscht*, Keyser, Munich, 1983, ch. 11, p. 166.
18 J. Bly, *Discovering Hallmarks on English Silver*, Shire Publications, Buckinghamshire, 8th edn., 1997, pp. 3–13.
19 J. Diviš, *Silber-Stempel aus aller Welt*, Battenberg Verlag, Augsburg, 1995, p. 39 (original title: *Značky Stříbra*, Aventinum Verlag, Prague, 1976).

Paper 9/00073I